

1. Intra- and Intermolecular Constraints

Condensed organic materials designed for nanotechnological applications are impacted significantly by internal and external constraints. Internal (intra- and intermolecular) constraints are inherent to the molecular architecture, and generally result from direct bonding, electrostatic interactions, or steric effects. Internal constraints can be incorporated *a priori* into molecular designs, as a prescription for desired material properties. This is illustrated in Fig. 1-1 with our work on organic non-linear optical (NLO) material systems for photonic application,⁴ where the “minuscule” flexibility difference in a intramolecular linker within a vast macromolecule is responsible for a significant alteration of the relaxational phase behaviour below the glass transition at $T_c = 77$ °C. Studies such as this, involving internal molecular constraints make an important aspect of our research. They involve novel sophisticated nano-tools and methodologies, and are carried out in parallel to material synthesis and recently also computer modelling.

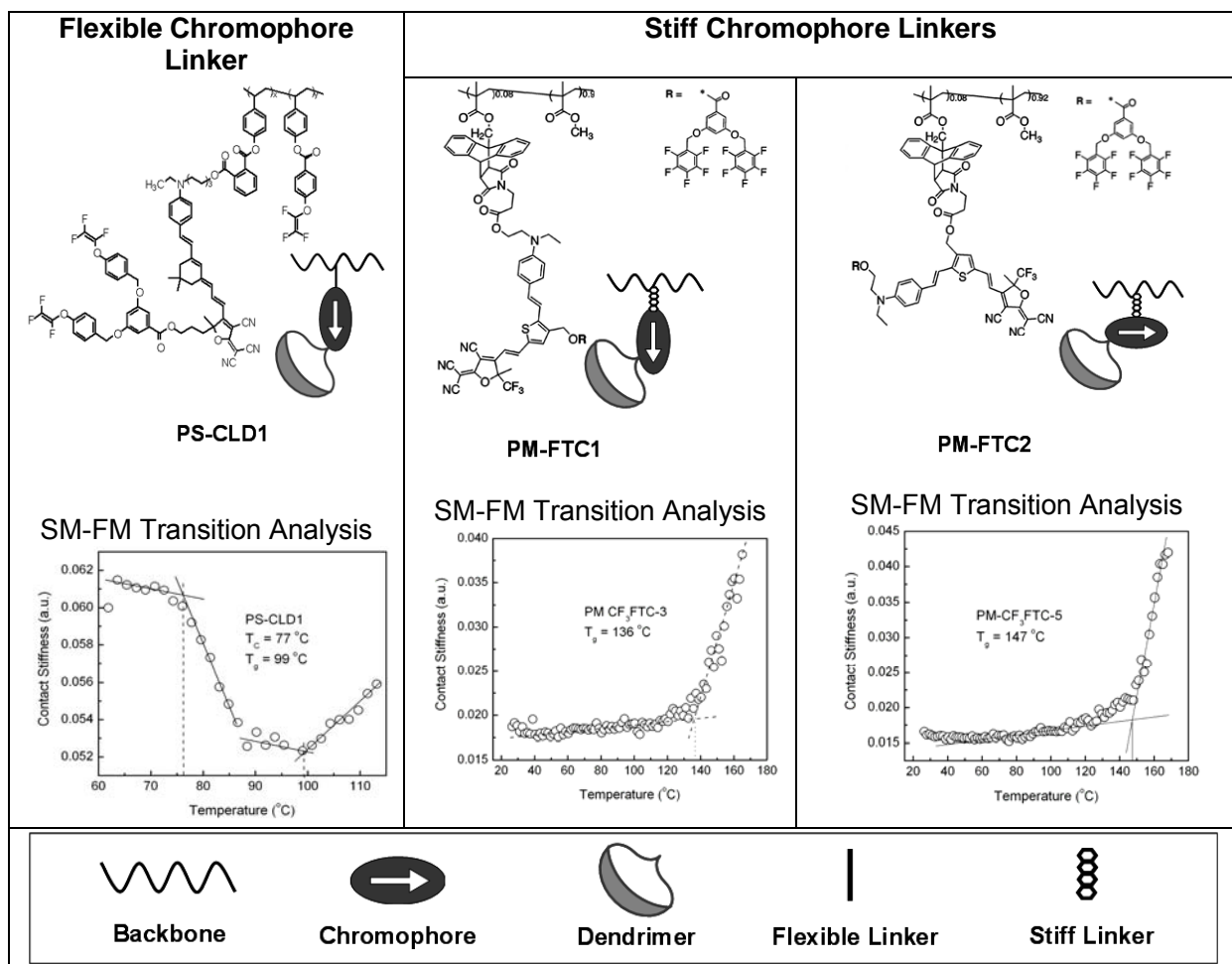


Fig. 1-1: Shear modulation force microscopy (SM-FM) analysis of side-chain dendronized NLO polymers. *Left:* PS-CLD1 with soft chromophore-backbone linker; *Right:* PM-FTC1 and PM-FTC2 with stiff linkers.⁴

Reflecting on effective material design concepts, a bottom-up molecular approach comes to mind, where, with the appropriate synthesis and under suitable processing conditions, materials are designed with desired properties and functionalities. The challenge is to anticipate bulk- or mesophase material properties from the molecular structure. This is generally approached in a reversed fashion by first analyzing the product, i.e. the condensed phase, and then pondering the possible molecular origin for specific properties. Depending on the specificity of the information gained experimentally, a molecular understanding is directly obtained, a molecular model is

developed, or a trial-and-error procedure is put in place. Once a molecular understanding (or a molecular model) for a specific class of materials is obtained, computer assisted molecular engineering can take place, and a wide variety of molecular structures and functionalities directed towards the material design objective can be tested. Thus, to excel from mere trial-and-error procedures and empiricism, experimental tools and methodologies have to be devised that provide direct access to nanoscale mobilities of constrained systems.

Over the past decade our group has pioneered various instrumental techniques that have provided insight into the nanoscale behaviour of constrained materials. In regards of inter- and intramolecular material intrinsic constraints, we introduced a method that is sensitive to the intrinsic friction process, not unlike the Stokes-Einstein friction mobility concept. Our method, referred to as *Intrinsic Friction Analysis (IFA)*,⁸ is based on lateral force microscopy⁹. With IFA, we have been studying the energetics and cooperativity of inter- and intramolecular mobilities that are available within well defined temperature windows, Fig. 1-2.

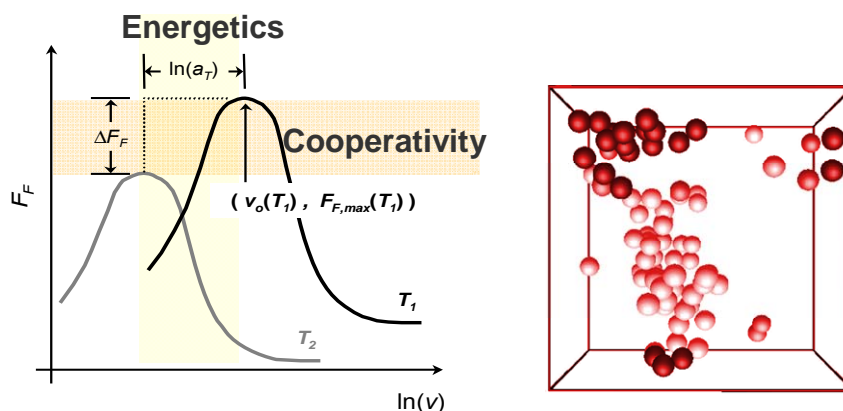


Fig. 1-2: *Left:* IFA schematic friction-velocity isotherms that if shifted accordingly (linear superposition principle) reveal energetic and cooperative information.^{1,8} *Right:* Schematic visualization of monomer clustering during a relaxation process. IFA combined with dielectric spectroscopy provides a direct method to determine the “cluster” length dimension that corresponds to computer simulations.⁸

Over the past few years, we have employed the IFA technique to a wide variety of materials to illuminate phenomenological processes from a submolecular perspective.^{1,3,4,8,10} Besides the fundamental analysis of transition phenomena, we have explored temporal and spatial cooperative phenomena and self-assembly mechanisms. Furthermore, IFA provided first truly molecular scale insight into the material intrinsic activation modes that are cause for energy dissipation during tribological sliding (c.f. subsection 3.1 below).

Some of our striking results involving IFA and other techniques are discussed in this section with specific foci on

- *enthalpic relaxation processes*, as found for side-chain relaxations in condensed organic matter,
- *entropic relaxation processes*, of particular relevance for glass forming materials, and
- *combined enthalpic and entropic processes*, discussed below on self-assembling molecular glasses.

1.1 Molecular Origin of Transition Phenomena – Enthalpic Processes

Transition analysis as conducted with differential scanning calorimetry, shear modulation force microscopy (SM-FM – discussed in greater detail below), electron spin resonance and other methods identify temperature regimes with critical boundaries (i.e., transition temperatures). To unravel underlying molecular mechanisms describing the transition in greater detail demands additional mobility analyses, such as dielectric spectroscopy, neutron reflectivity, or as addressed above, IFA. If

the material is confined to thin films, IFA is because of its high signal-to-noise ratio, the preferred technique. The insightful information towards a cognitive molecular design approach (versus trial-and-error) that can be obtained with IFA shall here be illustrated with our research on thin film polymeric NLO materials.⁶

As shown above, the dendronized side-chain NLO chromophore system PS-CLD1, Fig. 1-1, reveals a low temperature transition T_c at 77 °C. This transition turns out to be crucial for the acentric alignment of the dipolar chromophores, as it provides rotational mobility to the chromophore side-chain. The properties that are of foremost importance for organic NLO materials are the electro-optical (EO) activity that involves an acentric order of the chromophores, and temporal phase stability. One main approach in generating acentric order within NLO systems is to perform an electric field poling process, in which the randomly dispersed chromophores are aligned. For electric field poling, the glass transition temperature (T_g) is a key parameter with regard to both the *poling efficiency*, requiring high chromophore mobility often only available near T_g , and the *temporal stability* of the acentric order, demanding minimal chromophore mobility. These two contradicting factors make the molecular design of NLO systems challenging, requiring many levels of subtle adjustments for device optimization. The induced macroscopic nonlinearity is usually expressed with the electro-optical (E-O) coefficient r_{33} that is given as

$$r_{33} = \frac{|2N \cdot f(\omega) \cdot \beta \langle \cos^3 \theta \rangle|}{n^4} \quad (1.1)$$

where n is the refractive index, N is the chromophore number density, $f(\omega)$ is the local field factor, β is the second order hyperpolarizability, and $\langle \cos^3 \theta \rangle$ is the Boltzmann angle averaged order parameter.

Figure 1-3 illustrates the importance of the low temperature transition T_c . It can be inferred that the EO coefficient, r_{33} , significantly increased above T_c , thus, leading to an improved poling efficiency within T_c and T_g . The observed decrease in r_{33} above T_g can be attributed to a detrimental effect of excessive large scale mobility (in this case the polymer backbone translational motion) that leads to chromophore pairing, and thus, dipole annihilation. This study is witness to the subtle temperature dependence involving poling of organic NLO materials.

To provide insight into the origin for the beneficiary temperature window (T_c , T_g), we conducted a mobility analysis involving IFA. Figure

1-4 shows two distinct temperature regimes based on the activation energy signature (E_a). The two regimes are separated at the critical transition temperature T_c . The obtained values for the activation energies were comparable to the dendrimer mobility **A** and the rotational chromophore segmental motion **B** below and above T_c , respectively. If compared to the two other dendronized side-chain NLO chromophore systems PM-FTC1 and PM-FTC2, introduced in Figure 1-1, which lack a low temperature transition due to stiff side-chain linkages, the critical secondary relaxation at the flexible linkage **B** to the chromophore side-chain results, for PS-CLD1, in the desired chromophore mobility for electric field poling within the temperature window (T_c , T_g).

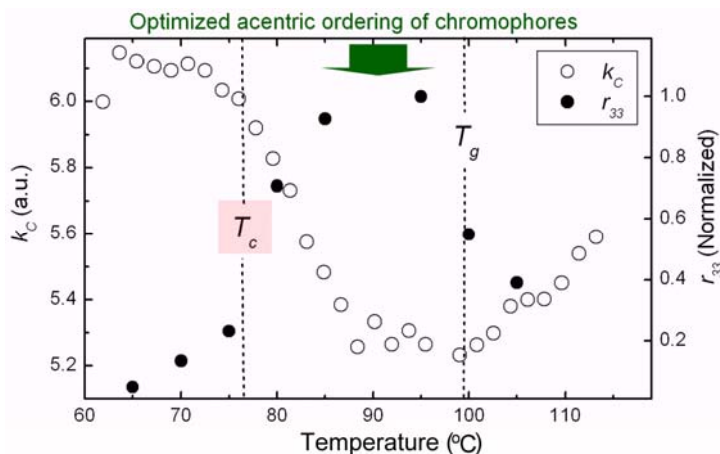
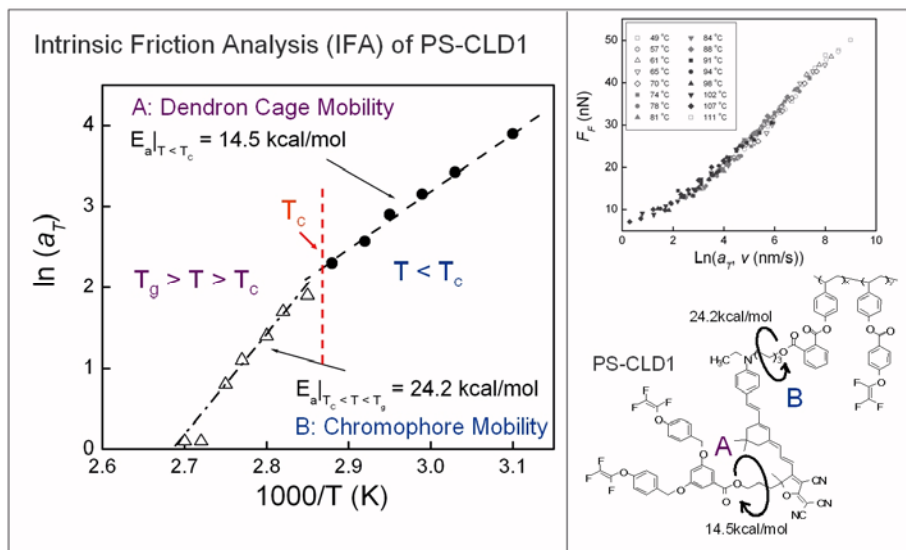


Fig. 1-3: SM-FM contact stiffness k_c data (●) from Fig. 1.1 in PS-CLD1 superimposed with corresponding EO activity coefficients, r_{33} (○). Optimized acentric ordering within T_c and T_g .⁶



This study illustrates the immense potential of IFA for investigating inter- and intramolecular mobilities in constrained and finite-size systems.

It is important to note that our discussion involving side-chain relaxations, considers enthalpic contributions to motion only. Contributions from entropic processes are discussed in the next section. Thermally activated enthalpic processes are time-temperature equivalent, i.e., time and temperature are equivalent to the extent that data (in our case friction) at one temperature can be superimposed on data at another temperature by shifting the curves (isothermal friction-velocity plots) by a_T along the log time axis to a single master curve as shown in Figure 1-4 (Right/Top). The set of horizontal shifts $\{a_T\}$, of friction-velocity isotherms, also referred to as thermal shift factors, provides the actual activation energies E_a , if plotted versus the inverse absolute temperature T , from

$$E_a = -R \left[\frac{\partial \ln(a_T)}{\partial (1/T)} \right]_p \quad (1.2)$$

R is the universal gas constant. This log-linear relationship is known as Arrhenius behavior. It should be noted that relaxation phenomena exist that are non-Arrhenius, as found for polymer rubbers above the glass transition temperature (c.f. sec. 1.2). In particular in nano-constrained systems, relaxation processes can also be highly cooperative, which leads to an entropic increase in the “apparent” activation energy.

1.2 Cooperativity During the Glass Forming Process – Entropic Processes

While non-cooperative processes, such as observed for side-chain relaxation, Fig. 1-4, are described in terms of the dynamic enthalpy ΔH^* alone, cooperative processes also include the dynamic entropy, ΔS^* , as given by the activation Gibbs free energy:

$$\Delta G^* = \Delta H^* - T\Delta S^* \quad (1.3)$$

Examples are long-range mobilities, such as the crankshaft motion in polymers during the glass forming process that yield strongly cooperative phenomena. Figure 1-2(Left) illustrates this in the IFA analysis that makes vertical shifting, ΔF_F , necessary to collapse the data to a single master curve. As derived by our group,¹ frictional vertical shifting, ΔF_F , can be related to the dynamic entropy via,

$$\Delta F_F \approx -\frac{T\Delta S^*}{\phi'} \quad (1.4)$$

where ϕ' is the contact area normalized stress activation volume. Thus, while horizontal shift factors, $\{a_T\}$, relate to the enthalpic behavior of the system, the vertical shift factors ΔF_F , relate to entropic cooperative behavior. The deconvolution of the two processes is inaccessible with conventional techniques but exclusive to IFA. Thus with direct access to the molecular mobility, we investigated the very complex process of glass forming.⁸

Since Adam and Gibbs (*J. Chem. Phys.* (1965) **43**, 139), structural relaxation near the glass transition has been visualized in terms of a correlated motion of polymer segments or domains, giving rise to dynamic heterogeneities. While the time scale of dynamic heterogeneities can be directly inferred from scattering experiments, the size of the cooperatively rearranging regions (typically 1-3 nm) is generally not directly obtainable and involves model assumptions. A nanoscopic description of polymer dynamics involves, in general, only two parameters: an appropriate macromolecular length scale and an internal, or monomeric, friction coefficient.

We employed IFA on a polymer rubber melt (polystyrene) close to its glass transition ($T_g = 373$ K), which resulted in the data presented in Figure 1-5(Left).⁸ The log-linear averaged activation energy of ~ 90 kcal/mol coincides well with the apparent activation energy for the α -relaxation process. Matching the relaxation peaks obtained by a dielectric relaxation spectroscopy (DRS) with the IFA peaks, the cooperation length can be experimentally determined via

$$X_d(T) = v_o(T) \cdot \tau_\alpha(T) \quad (1.5)$$

where $v_o(T)$ is the velocity corresponding to the α -peak of the $F_F(v)$ curves (IFA), and $\tau_\alpha(T)$ is the α -relaxation time from DRS. The cooperation lengths $X_d(T)$ were determined with $v_o(T)$ and equation (1.5) so that the resulting α -relaxation times are consistent with those from dielectric spectroscopy, Fig. 1-5(Right). It is important to note that the determination of the length scale of cooperativity did not involve any of the many theoretical models, which makes this experimental methodology unique. The “uniqueness” goes even a step further, as our experimental work can actually be matched to theoretical models involving mode coupling theories and molecular dynamic simulations.⁸

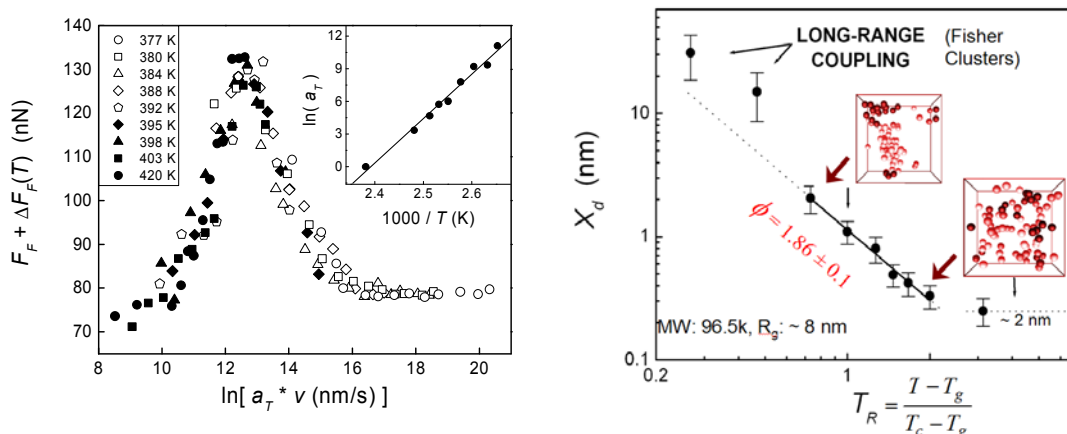


Fig. 1-5: Left: IFA of polystyrene (MW: 06.5k) above T_g . Right: IFA/DRS provides a direct measure of the cooperation length X_d as function of the reduced temperature T_R . $T_c = T_g + 15$ °C is the crossover temperature – an experimental observable at vanishing ΔF_F . The slope ϕ has been theoretically confirmed with a molecular dynamic (MD) simulation.⁸

This study illustrates our efforts in studying highly cooperative phenomena. We have recently devised a method to determine the entropic component from vertical ΔF_F shifts utilizing the following relationship:^{1,4}

$$E_a = RT_R [1 + \ln(k_B T_R / 2\pi\hbar f_R)] + T \Delta S \quad (1.6)$$

based on the apparent activation energy E_a of the underlying intrinsic friction dissipation process, the universal gas constant R , the relaxation peak frequency f_R , the activation entropy ΔS , the relaxation temperature T , the Boltzmann constant k_B , and the Plank constant h . For a purely activated dissipation process, i.e., a process without cooperativity, the entropic term $T\Delta S$ vanishes. An example for such a process is the γ -relaxation in *PS* (further discussed in 3.1), where the side-chain phenyls rotate independently from one another. The degree of cooperativity can be directly inferred from the vertical shift contribution ΔF_F required to obtain a single master curve, as per Eq. 1.4, and as illustrated in Figure 1.6 for polystyrene above (α -relaxation) and below (β -relaxation) the glass transition temperature. Our experiments show that the cooperative energy contribution $T_R \Delta S$ to the

total apparent energy can be very significant (e.g., 80% and 20 %, respectively, for the two mentioned relaxations). Considering that in nanoscale confined systems cooperative effects can be expected to be appreciably enhanced due to finite size and interfacial constraints, it is imperative that studies of this kind are of great value not only from a fundamental but also engineering perspective.

To close this discussion, it shall be pointed out that IFA also provides insight into non-Arrhenius processes that are also of great importance for nano-constrained materials. This is here briefly illustrated with the rubbery state of polystyrene close to the glass transition temperature. The non-linear log-behavior of the shift factors $\{a_T\}$ is typically treated with the Williams-Landel-Ferry (WLF) expression

$$\Delta E_a = 2.303 \cdot R \cdot c_1 \cdot c_2 \cdot \frac{T^2}{(c_2 + T - T_0)^2} \quad (1.7)$$

As shown in Figure 1-7, IFA results are well fitted by the WLF generalized model with fitting parameters that correspond well to state-of-the-art methods.¹⁰

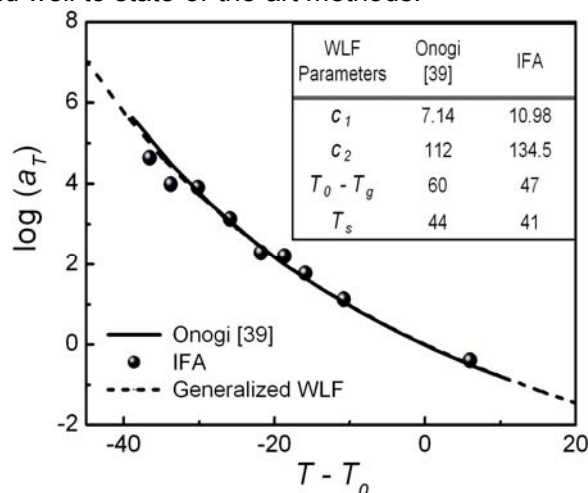


Fig. 1-7: The shift factor plotted against reduced temperature for rubbery polystyrene and Ferry's generalized WLF curve Inset: WLF parameters from literature and IFA.¹⁰

To close this aspect of our review, we found that IFA is well suited for analyzing the molecular mobility close to interfaces, and in thin films. As a local probe, IFA is also well suited for investigating laterally heterogeneous materials, such as phase separated systems (e.g., polymer blends). From a fundamental perspective, we recognized the importance of entropic constraints, in both value and preponderance in internal molecular and external nanoconstrained systems.

1.3 Self-Assembly Processes – Combined Enthalpic and Entropic Processes

In the prior discussion, I provided some insight into our group's research on analyzing inter- and intra-molecular mobilities of molecularly or interfacially constrained systems based on enthalpic

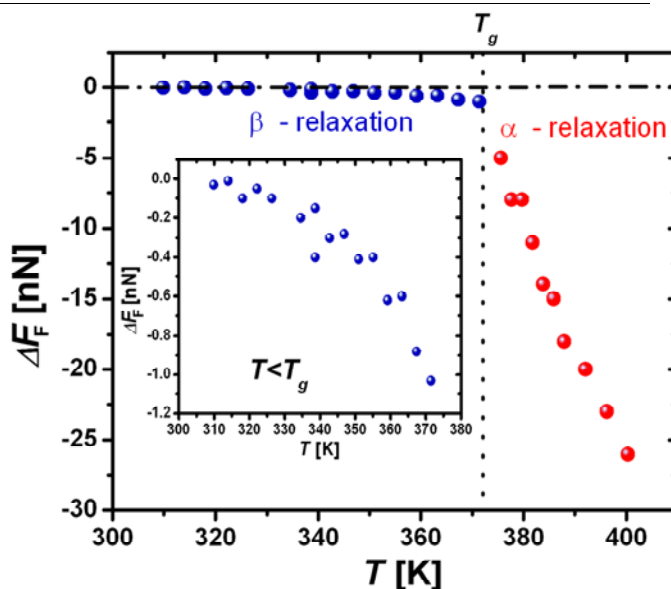


Figure 1-6: Vertical IFA friction shift ΔF_F of polystyrene – a measure of the degree of cooperativity - reveals a significant entropic contribution to the apparent activation energy.¹

activation barriers and entropic cooperative rearrangements. Of particular interest to us is the study of combined enthalpic and entropic processes, with focus on a wide variety of material systems (e.g., organic monolayer systems, ultrathin organic films, interfacially constrained polymers, and nanocomposites), and technological applications (e.g., organic membrane separation, tribology and adhesion, and energy production and storage) with focus on fundamental aspects (e.g., confined flow and relaxations, submolecular energy dissipation phenomena, local mechanical and electronic transport properties, and constrained phase behaviours).

Of particular interest to us are organic systems that are "imperfect" such as amorphous systems with local order. Although the current research efforts of many groups focus primarily on organic self-assembled crystalline systems, we believe that, by looking at living or organic matter, less perfect molecular arrangements have a higher potential due to increased resiliency. For instance, in organic materials, detrimental effects caused by defects are significantly less pronounced than in crystalline materials. Also, increased molecular mobility in organic

amorphous systems, due to intrinsically lower potential barriers compared to crystalline systems, offer increased possibilities towards engineering applications. This aspect has been demonstrated, for instance, just recently in organic electronics, Figure 1-8, involving self-assembling NLO molecular glasses that yield, with over 300 pm/V, the highest ever reported EO activity

Dealing with organic or biological systems makes us particularly aware of the subtle but important differences. Weak interactions with bonding strengths small compared to kT are of immense importance as they dictate local mobilities. As such, one has to consider to what degree these processes are cooperative on a molecular scale. Highly cooperative phenomena, as those found in glass forming processes, as discussed above, exhibit unusually large apparent activation energies of up to 100 kcal/mol that are indicative of a high degree of complexity in the motion associated with relaxations. Weak interactions play an important role in self-assembled NLO molecular glasses, with structures of high cooperativity that lead to extraordinary increases in, for instance, EO activity – an aspect that is here a little further discussed.

The remarkable increase in EO activity beyond 300 pm/V (Fig. 1-8) is tribute to a new class of NLO materials of self-assembling molecular glasses (HDFD; Fig. 1-9) involving quadrupolar phenyl-perfluorophenyl (Ph-Ph^{F}) interactions. Although, self-assemblies from Ph-Ph^{F} interactions have been reasonably well-known in material chemistry for many years, and employed for optoelectronic and liquid crystalline materials, its breakthrough as NLO materials has just recently occurred with HDFD.³

HDFD, the most basic representative of this new class of self-assembling NLO materials takes advantage of the strong affinity between phenyl (Ph) and perfluorophenyl (Ph^{F}) moieties, which form face-to face Ph-Ph^{F} stacks of alternating hydrocarbon and perfluorinated moieties due to their complementary quadrupole moments. Both Ph and Ph^{F} moieties are integrated in second generation Fréchet-type dendrimers, which then are incorporated as peripheral dendrons on the π -bridge and the donor-end of the NLO chromophores to allow the chromophores to form an ordered network, as illustrated in Figure 1-9.

Figure 1-9 provides the chemical structure of HDFD, where HD and FD stand for the Ph-dendrimer and Ph^{F} -dendrimer, respectively. Based on the quadrupolar Ph-Ph^{F} interaction and the

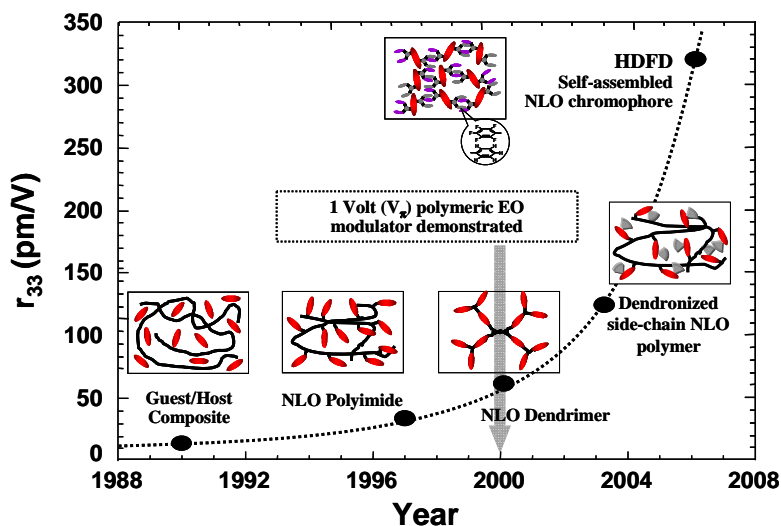


Figure 1-8: Progress in designing high EO activity with organic NLO material.³

measured ultrahigh EO activities of over 300 pm/V, one is tempted to visualize the self-aggregation processes as highly ordered. However, X-ray analysis indicates that the structure is amorphous. Thus, the orientational stability in this system originates from a mesoscale structural alignment, i.e., a networking system that resembles a polymer chain, Figure 1-9. The obtained high acentric order of the chromophores after electric field poling suggests a network system that contrary to conventional polymers is highly temperature susceptible. Chains can be either broken, reconnected, or can form new connections under appropriate temperature conditions. This highly complex dynamic system exhibits inter-molecular relaxations with enthalpic activation barriers and cooperative phenomena.

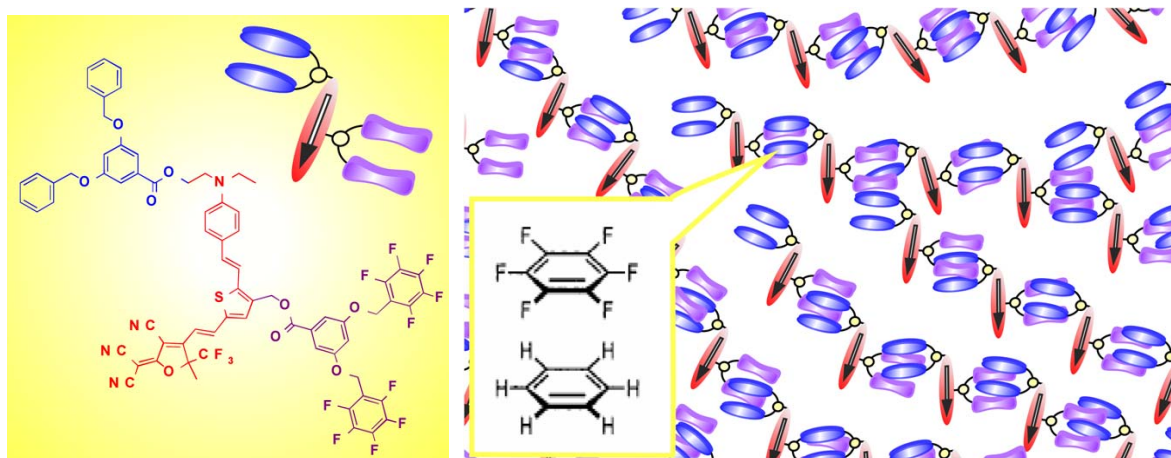


Fig. 1-9: HDFD – a glass forming chromophore containing molecule with phenyl and pentafluorophenyl rings incorporated as peripheral dendrons on the π -bridge and the donor-end of the chromophores. “Polymerized” self-assembly networking model visualizing the dynamics in intact or broken chains.³

To investigate the subtle dynamics and energetics of the HDFD condensed phases, we utilized in principle two microscopic methodology, i.e., IFA and shear modulation force microscopy (SM-FM), which will be introduced below, wherein the scanning probe microscopy (SPM) cantilever is used as a thermomechanical (TM) sensor to detect critical temperature transition values.³ Guided by SM-FM, IFA was conducted in three temperature regimes defined by the two transition temperatures T_1 and T_2 . IFA results are presented in Figure 1-10 in regards of both the energetics and cooperativity.

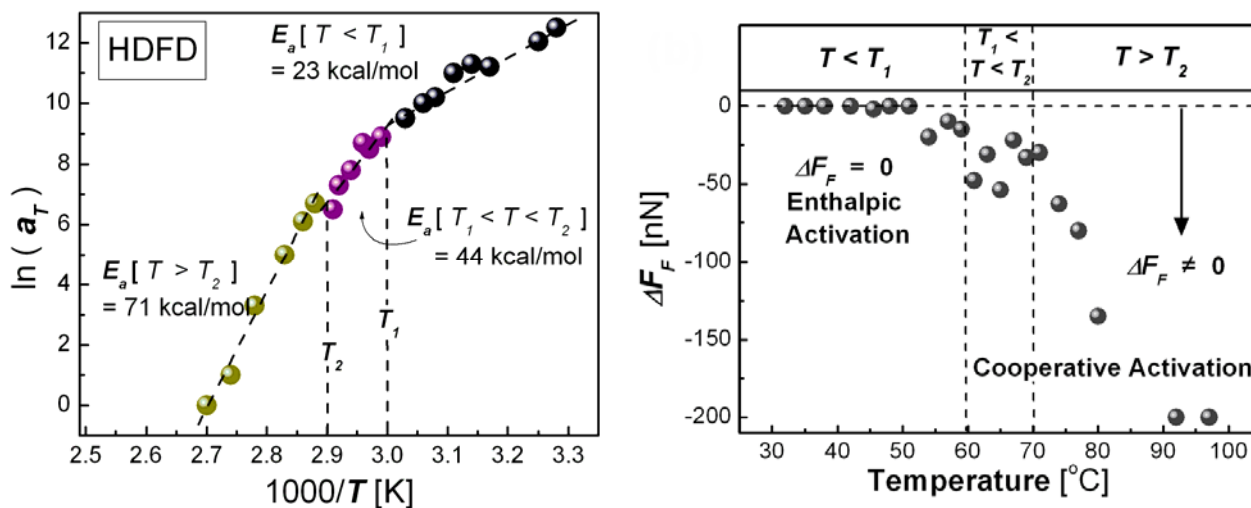

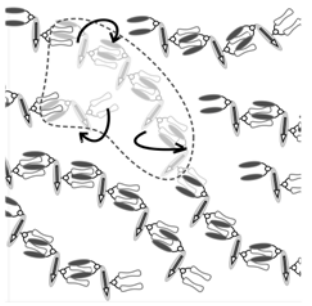



Fig. 1-10: (Left) a_T -shift-factor analyses in three temperature regimes of HDFD with apparent activation energies. (Right) Vertical shift, ΔF_F as a function of temperature for HDFD. Entropic (cooperative) contribution is noticeable above T_1 .³

Based on the information collected and knowledge of face-to-face phenyl/per-fluorophenyl interactions, the dynamics and cooperativity in the HDFD system can be interpreted as follows, Table 1-1.³

- Below T_1 , the activation energy is associated with the dissociation of Ph-Ph^F pairs that take place randomly in isolated events. It describes the uncorrelated molecular decoupling process of the glassy state of HDFD.
- In the intermediate temperature range ($T_1 < T < T_2$), an increase in the density of dissociation sites leads to a cooperative phenomena, where molecules move in registry.
- Above but still close to T_2 , the assembly breaks down but the molecular building blocks still possess high cooperativity, typical of a polymer melt close to the glass transition.

Table 1-1: Activation Energy and Cooperativity in HDFD.³

$T < T_1$	$T_1 < T < T_2$	$T_2 < T$
$E_a = 23 \text{ kcal/mol}$	$E_a = 44 \text{ kcal/mol}$	$E_a = 71 \text{ kcal/mol}$
$T\Delta S^* \approx 0$	$T\Delta S^* = 26-30 \text{ kcal/mol}$	$T\Delta S^* = 52-56 \text{ kcal/mol}$
		
Uncorrelated molecular decoupling in “glass state”	Cooperative decoupling	High cooperativity in “melt state”

Thus, while the dynamic enthalpy, i.e., the dissociation of Ph-Ph^F pairs in HDFD, reflects a common relaxation mechanism for all three phases, the dynamic entropy exposes the phase variations in terms of cooperativity. With the introduced nanoscale thermomechanical methodology, it is now possible to study entropic phenomena of other molecular structures of self-assembled glass forming NLO system with, for instance, more or less flexible dendrons or larger Ph and Ph^F moieties. This is research that is currently on-going in our laboratory.

Being able to deconvolute and quantify isolated processes from cooperative relaxation processes in condensed materials, our research efforts involving IFA and complementary techniques have shown to provide fundamental insight into the complexity of inter- and intramolecular constrained systems, which in turn provided the necessary input to design material cognitively. In the following section, we will shift from material specific constraints to our research on externally imposed constraints, such as interfacial and dimensional constraints.

6. References and Citations Therein

- ¹ D. B. Knorr, T. Gray, and R. M. Overney, *Cooperative and Submolecular Dissipation Mechanisms of Sliding Friction in Complex Organic Systems*, J. Chem. Phys. **129**, 074504 (2008).
- ² M. Y. He, A. S. Blum, G. Overney, and R. M. Overney, *Effect of interfacial liquid structuring on the coherence length in nanolubrication*, Physical Review Letters **88**, 154302 (2002).
- ³ T. Gray, T. D. Kim, D. B. Knorr, J. D. Luo, A. K. Y. Jen, and R. M. Overney, *Mesoscale dynamics and cooperativity of networking dendronized nonlinear optical molecular glasses*, Nano Letters **8**, 754-9 (2008).
- ⁴ D. B. Knorr, T. Gray, and R. M. Overney, *Intrinsic Friction Analysis - Novel Nanoscopic Access to Molecular Mobility in Constrained Organic Systems*, Ultramicroscopy **in press** (2008).
- ⁵ R. M. Overney, E. Meyer, J. Frommer, D. Brodbeck, R. Luthi, L. Howald, H. J. Guntherodt, M. Fujihira, H. Takano, and Y. Gotoh, *Friction Measurements on Phase-Separated Thin-Films with a Modified Atomic Force Microscope*, Nature **359**, 133-5 (1992).
- ⁶ T. Gray, R. M. Overney, M. Haller, J. Luo, and A. K. Y. Jen, *Low temperature relaxations and effects on poling efficiencies of dendronized nonlinear optical side-chain polymers*, Applied Physics Letters **86** (2005).
- ⁷ S. Sills, R. M. Overney, W. Chau, V. Y. Lee, R. D. Miller, and J. Frommer, *Interfacial glass transition profiles in ultrathin, spin cast polymer films*, Journal of Chemical Physics **120**, 5334-8 (2004).
- ⁸ S. Sills, T. Gray, and R. M. Overney, *Molecular dissipation phenomena of nanoscopic friction in the heterogeneous relaxation regime of a glass former*, Journal of Chemical Physics **123** (2005).
- ⁹ R. Overney and E. Meyer, *Tribological Investigations Using Friction Force Microscopy*, Mat. Res. Soc. Bulletin **18**, 26-34 (1993).
- ¹⁰ T. Gray, J. Killgore, J. D. Luo, A. K. Y. Jen, and R. M. Overney, *Molecular mobility and transitions in complex organic systems studied by shear force microscopy*, Nanotechnology **18** (2007).
- ¹¹ R.M. Overney and S. E. Sills, in *Interfacial Properties on the Submicron Scale*, edited by J. Frommer and R. M. Overney (Oxford Univ. Press, New York, 2001), p. 2-23.
- ¹² R. M. Overney, D. P. Leta, L. J. Fetters, Y. Liu, M. H. Rafailovich, and J. Sokolov, *Dewetting dynamics and nucleation of polymers observed by elastic and friction force microscopy*, Journal of Vacuum Science & Technology B **14**, 1276-9 (1996).
- ¹³ R. M. Overney, G. Tindall, and J. Frommer, in *Handbook of Nanotechnology*, edited by B. Bhushan (1439-1453, Heidelberg, 2007).
- ¹⁴ S. R. Ge, L. T. Guo, M. H. Rafailovich, J. Sokolov, R. M. Overney, C. Buenviaje, D. G. Peiffer, and S. A. Schwarz, *Wetting behavior of graft copolymer substrate with chemically identical homopolymer films*, Langmuir **17**, 1687-92 (2001).
- ¹⁵ A. Karim, T. M. Slawacki, S. K. Kumar, J. F. Douglas, S. K. Satija, C. C. Han, T. P. Russell, Y. Liu, R. Overney, O. Sokolov, and M. H. Rafailovich, *Phase-separation-induced surface patterns in thin polymer blend films*, Macromolecules **31**, 857-62 (1998).
- ¹⁶ C. Buenviaje, S. R. Ge, M. Rafailovich, J. Sokolov, J. M. Drake, and R. M. Overney, *Confined flow in polymer films at interfaces*, Langmuir **15**, 6446-50 (1999).
- ¹⁷ R. M. Overney, C. Buenviaje, R. Luginbuhl, and F. Dinelli, *Glass and structural transitions measured at polymer surfaces on the nanoscale*, Journal of Thermal Analysis and Calorimetry **59**, 205-25 (2000).
- ¹⁸ S. Ge, Y. Pu, W. Zhang, M. Rafailovich, J. Sokolov, C. Buenviaje, R. Buckmaster, and R. M. Overney, *Shear modulation force microscopy study of near surface glass transition temperatures*, Physical Review Letters **85**, 2340-3 (2000).
- ¹⁹ E. Meyer, R. Overney, R. Luthi, D. Brodbeck, L. Howald, J. Frommer, H. J. Guntherodt, O. Wolter, M. Fujihira, H. Takano, and Y. Gotoh, *Friction Force Microscopy of Mixed Langmuir-Blodgett-Films*, Thin Solid Films **220**, 132-7 (1992).
- ²⁰ E. Meyer, R. Overney, D. Brodbeck, L. Howald, R. Luthi, J. Frommer, and H. J. Guntherodt, *Friction and Wear of Langmuir-Blodgett-Films Observed by Friction Force Microscopy*, Physical Review Letters **69**, 1777-80 (1992).
- ²¹ L. Howald, R. Luthi, E. Meyer, G. Gerth, H. G. Haefke, R. Overney, and H. J. Guntherodt, *Friction Force Microscopy on Clean Surfaces of NaCl, NaF, and AgBr*, Journal of Vacuum Science & Technology B **12**, 2227-30 (1994).
- ²² R. M. Overney, T. Bonner, E. Meyer, M. Reutschi, R. Luthi, L. Howald, J. Frommer, H. J. Guntherodt, M. Fujihira, and H. Takano, *Elasticity, Wear, and Friction Properties of Thin Organic Films Observed with Atomic-Force Microscopy*, Journal of Vacuum Science & Technology B **12**, 1973-6 (1994).

- ²³ R. M. Overney, H. Takano, M. Fujihira, W. Paulus, and H. Ringsdorf, *Anisotropy in Friction and Molecular Stick-Slip Motion*, Physical Review Letters **72**, 3546-9 (1994).
- ²⁴ R. M. Overney, H. Takano, and M. Fujihira, *Elastic Compliances Measured by Atomic-Force Microscopy*, Europhysics Letters **26**, 443-7 (1994).
- ²⁵ R. M. Overney, H. Takano, M. Fujihira, E. Meyer, and H. J. Guntherodt, *Wear, Friction and Sliding Speed Correlations on Langmuir-Blodgett-Films Observed by Atomic-Force Microscopy*, Thin Solid Films **240**, 105-9 (1994).
- ²⁶ F. Dinelli, C. Buenviaje, and R. M. Overney, *Glass transitions of thin polymeric films: Speed and load dependence in lateral force microscopy*, Journal of Chemical Physics **113**, 2043-8 (2000).
- ²⁷ C. Buenviaje, F. Dinelli, and R. M. Overney, *Investigations of heterogeneous ultrathin blends using lateral force microscopy*, Macromolecular Symposia **167**, 201-12 (2001).
- ²⁸ S. Sills and R. M. Overney, *Creeping friction dynamics and molecular dissipation mechanisms in glassy polymers*, Physical Review Letters **91**, 095501 (2003).
- ²⁹ S. Sills, H. Fong, C. Buenviaje, M. Sarikaya, and R. M. Overney, *Thermal transition measurements of polymer thin films by modulated nanoindentation*, Journal of Applied Physics **98** (2005).
- ³⁰ S. Sills, T. Gray, J. Frommer, and R. M. Overney, in *Applications of Scanned Probe Microscopy to Polymers*, (2005), Vol. 897, p. 98-111.
- ³¹ S. Sills, R. M. Overney, B. Gotsmann, and J. Frommer, *Strain shielding and confined plasticity in thin polymer films: Impacts on thermomechanical data storage*, Tribology Letters **19**, 9-15 (2005).
- ³² J. P. Killgore and R. M. Overney, *Interfacial mobility and bonding strength in nanocomposite thin film membranes*, Langmuir **24**, 3446-51 (2008).
- ³³ R. M. Overney, D. P. Leta, C. F. Pictroski, M. H. Rafailovich, Y. Liu, J. Quinn, J. Sokolov, A. Eisenberg, and G. Overney, *Compliance measurements of confined polystyrene solutions by atomic force microscopy*, Physical Review Letters **76**, 1272-5 (1996).
- ³⁴ M. Y. He, A. S. Blum, D. E. Aston, C. Buenviaje, R. M. Overney, and R. Luginbuhl, *Critical phenomena of water bridges in nanoasperity contacts*, Journal of Chemical Physics **114**, 1355-60 (2001).
- ³⁵ S. Sills, K. Vorvolakos, M.K. Chaudhury, and R. M. Overney, in *Friction and Wear on the Atomic Scale*, edited by E. Gnecco and E. Meyer (Springer Verlag, Heidelberg, 2007), p. 659-76.
- ³⁶ E. Meyer, L. Howald, R. M. Overney, H. Heinzelmann, J. Frommer, H. J. Guntherodt, T. Wagner, H. Schier, and S. Roth, *Molecular-Resolution Images of Langmuir-Blodgett-Films Using Atomic Force Microscopy*, Nature **349**, 398-400 (1991).
- ³⁷ R. Luthi, R. M. Overney, E. Meyer, L. Howald, D. Brodbeck, and H. J. Guntherodt, *Measurements on Langmuir-Blodgett-Films by Friction Force Microscopy*, Helvetica Physica Acta **65**, 866-7 (1992).
- ³⁸ F. Schabert, A. Hefti, K. Goldie, A. Stemmer, A. Engel, E. Meyer, R. Overney, and H. J. Guntherodt, *Ambient-Pressure Scanning Probe Microscopy of 2d Regular Protein Arrays*, Ultramicroscopy **42**, 1118-24 (1992).
- ³⁹ J. Frommer, R. Luthi, E. Meyer, D. Anselmetti, M. Dreier, R. Overney, H. J. Guntherodt, and M. Fujihira, *Adsorption at Domain Edges*, Nature **364**, 198- (1993).
- ⁴⁰ R. M. Overney, E. Meyer, J. Frommer, H. J. Guntherodt, M. Fujihira, H. Takano, and Y. Gotoh, *Force Microscopy Study of Friction and Elastic Compliance of Phase-Separated Organic Thin-Films*, Langmuir **10**, 1281-6 (1994).
- ⁴¹ R. M. Overney, manuscript in preparation.
- ⁴² T. Gray, C. Buenviaje, R. M. Overney, S. A. Jenekhe, L. X. Zheng, and A. K. Y. Jen, *Nanorheological approach for characterization of electroluminescent polymer thin films*, Applied Physics Letters **83**, 2563-5 (2003).
- ⁴³ T. D. Kim, J. W. Kang, J. D. Luo, S. H. Jang, J. W. Ka, N. Tucker, J. B. Benedict, L. R. Dalton, T. Gray, R. M. Overney, D. H. Park, W. N. Herman, and A. K. Y. Jen, *Ultralarge and thermally stable electro-optic activities from supramolecular self-assembled molecular glasses*, Journal of the American Chemical Society **129**, 488-9 (2007).
- ⁴⁴ J. H. Wei, M. Y. He, and R. M. Overney, *Direct measurement of nanofluxes and structural relaxations of perfluorinated ionomer membranes by scanning probe microscopy*, Journal of Membrane Science **279**, 608-14 (2006).
- ⁴⁵ J. P. Killgore, W. King, K. Kjoller, and R. M. Overney, *Heated-tip AFM: Applications in Nanocomposite Polymer Membranes and Energetic Materials*, Microscopy Today **15**, 20-5 (2007).